Analytical Methods

Accepted Manuscript

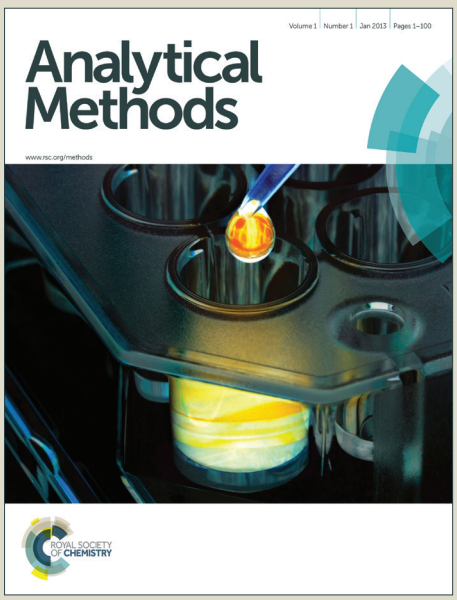

ROYAL SOCIETY OF CHEMISTRY

www.rsc.org/methods

Age-related changes in functional connectivity between young adulthood and late adulthood

Xin Xu[1], Qifan Kuang[2], YongQing Zhang[3], HuiJun Wang[2], Zhining Wen[2] and Menglong Li[2§]

[1]College of Life Science, Sichuan University, Chengdu, 610064, China

[2] College of Chemistry, Sichuan University, Chengdu, 610064, China

[3] College of Computer Science, Sichuan University, Chengdu, 610064, China

[§]Corresponding author

Email addresses:

XX: xuxinperfect@gmail.com

QK: littlestudent@163.com

YZ: zhangyongqingscu@hotmail.com

HW: prettywhj@163.com

ZW:w_zhining@163.com

ML: liml@scu.edu.cn

No.29 Jiuyanqiao Wangjiang Road, Chengdu, 610064

Tel: +86 28 85413330

Abstract

Recently, age-related changes in functional connectivity have gained more attentions in an attempt to investigate the functional changes across development. In this study, we examined functional connectivity, as derived from resting state functional magnetic resonance imaging (R-fMRI), in 90 cortical and subcortical regions for two healthy groups in young adulthood (ages 18-28 y) and late adulthood (ages 63-73 y). Comparing the process for constructing a functional network, we found that the network in young adulthood was more easily fully connected than that in late adulthood', indicating that the central regions, frontal lobe, parietal lobe and limbic lobe possibly occupy more resources in late adulthood. We confirmed that both the young adulthood' and late adulthood' brain had a "small-world" organization, and that there was a further loss of small-world characteristics in late adulthood. Additionally, we found that late adulthood exhibited a more social-like organization of the brain functional network than young adulthood. Further, connectivity density showed a general decrease in most brain areas, but only the temporal lobe and occipital lobe showed a decrease in connectivity strength in late adulthood. Conversely, the parietal lobe showed an increase in connectivity density in late adulthood. Our study provides additional support for elucidating the functional changes of the brain across development, and characterizing these changes will lead to a better understanding of the cognitive decline that occurs with advanced aging.

1. Introduction

Normal aging is a complicated biological phenomenon and is accompanied by cognitive decline. In general, ageing is characterized by a progressive loss of muscle, working memory, executive

function and by motor impairment, etc. [1]. As the brain is one of the most sophisticated and important organs, its aging has naturally drawn wide public attention. Especially in recent decades, anatomical and functional neuroimaging techniques such as diffusion tensor imaging (DTI), functional MRI (fMRI), electroencephalography (EEG), magnetoencephalography (MEG), etc. have been widely applied to brain research; for a review, see Ed Bullmor and Olaf Sporns [2]. Structural image studies examining the development of white-matter pathways have reported an increase in anisotropy and a decrease in the overall diffusion in major white-matter fiber tracts. Functional image studies have also shown that connectivity and network integrity decline with age [3-5].

Resting-state functional connectivity MRI (R-fMRI) is widely acknowledged to be a powerful technique for investigating the functional organization of the human brain. This method was applied to exploring brain functional connectivity, through detecting associated changes in blood flow, based on the spontaneous low-frequency (< ~0.1 Hz) blood oxygen level dependent (BOLD) signal fluctuations found in some correlated brain regions. Commonly, these low frequency BOLD fluctuations have been reported to be of physiological importance and have been suggested to relate to spontaneous neural activity [6,7]. A rapidly growing number of studies adopting this BOLD method have investigated the age-related functional changes of the human brain with the use of graph theory. In the context of a graph, brain regions (voxel/area) are described by nodes and connections, structurally denoting anatomical links. Functionally, the symmetrical statistical association or dependency between elements is referred to as edges on the graph. A recent study by Detsje and colleagues of childhood and young adult development investigated whole-brain functional connectivity using independent component analysis (ICA). They reported that both children and young adults showed similar spatial patterns of functionally connected regions and that the strength of the functional connectivity between brain regions was significantly different in these two groups [8]. Previous studies of development have reported that from childhood to adulthood, there was a general decrease in correlation strength between regions close in anatomical space but an increased correlation strength between selected regions distant in space; although, the functional brain network of both showed “small-world” properties [9,10]. The use of graph theory along with R-fMRI to characterize the organization of complex networks provided a useful approach for investigating the brain functional network in normal human aging.

Small-world networks, as characterized by high clustering and short path length, were originally proposed by Watts and Strogatz [11]. It was revealed that the small-world metrics derived from R-fMRI, MEGs and EEGs data could describe the integrated and special functional organization of the human brain [12-14]. Furthermore, the effects of normal aging, development and neurological diseases on small-world networks have been largely assessed with R-fMRI. In prior studies, it was reported that functional brain networks showed a loss of small-world properties in Alzheimer’s disease [15,16], disrupted small-world networks in schizophrenia [17,18] and altered quantitative values in the global properties in major depressive disorder (MDD) [19]. In addition, previous work examined the small-world metrics between children and young adults, with both showing “small-world” like properties that are significantly different in their hierarchical organization and interregional connectivity [9,10]. However, only a small number of studies have compared the small-world metrics between young adulthood and late adulthood. A few recent studies have shown that age impairs the economical performance of small-world brain networks [20,21]. One of the goals of the present study was to lend more support to these findings. Over a

wide range of sparsity values, we examined the small-world properties between young adulthood and late adulthood using several datasets to validate whether all the young adulthood groups could be significantly distinguished from the late adulthood group.

Previous studies suggested that analyzing the degree correlations of a network could predict the modularity, and it was also reported that the assortative mixing in task-related brain activation showed a positive correlation between a node's degree and the average of its direct neighbors' degrees [22,23]. Luca and his colleagues reported that in brain functional connectivity maps, the highly connected nodes tend to link to other highly connected nodes [24]. To our knowledge, the degree correlation between young adulthood and late adulthood has not yet been investigated. Additionally, there were several studies investigating the strength of region inter-connectivity, brain activity and functional connectivity between young adulthood and late adulthood. These studies suggested that there was a tendency toward reduced resting-state brain activity in the 'default-mode' network (DMN)[25,26], decreased modularity and decreased local efficiency [27,28]. However, few studies have explored these comparisons from perspective of the process of constructing functional networks. Therefore, we attempt to address this issue by using our method and expect to provide more information about normal aging.

In the current study, 1) we investigated the brain functional connectivity in young adulthood (18 ~ 26 years) and late adulthood (63 ~ 73 years) during the process of constructing fully connected functional networks; 2) we explored the small-world properties between groups with one late adulthood group and several young adulthood groups from different laboratories; 3) we examined the social-like organization of the brain functional network, using the approach described by Eguiluz et al.; and 4) we further examined the connectivity density and connectivity strength within anatomically distinct brain areas between these groups. As numerous studies have examined the intrinsically distinct functional networks, e.g., auditory, PCC/vmPFC, language, primary visual cortex and especially DMN using R-fMRI [29], we explored the functional networks within anatomically distinct brain areas. In general, we expected to find different patterns of functional connectivity between young adulthood and late adulthood.

2. Materials and methods

2.1 Ethics statement

We performed our analyses on publicly available imaging data from the 1000 Functional Connectomes Project (all data are available at http://fcon_1000.projects.nitrc.org). TRT reliability was assessed on the NYU TRT dataset. The corresponding institutional review boards approved or provided waivers for the submission of anonymized data, which were obtained with written informed consent from each participant.

2.2 Data

All the data used in this study were selected from the 1000 Functional Connectomes Project (http://fcon_1000.projects.nitrc.org/), the purpose of which is to provide a large-scale functional imaging dataset through collecting resting-state functional magnetic resonance imaging (R-fMRI) datasets from its member sites around the world. This study included 229 healthy young adults from Zang, Y.F. (n = 198, ages 18 ~ 26, 76M/122F) and Rombouts, S.A.R.B (n = 31, ages 18 ~ 28, 23M/8F) and 16 late adulthood from Sorg, C./Riedel, V. (n = 16, ages 63~73, 10M/6F). After pre-

processing, 206 subjects were finally selected to be analyzed in the following sections. All the neural images were acquired from right-handed subjects who were guided to lie down without moving, close their eyes, and to not think of anything but to stay awake.

2.3 Pre-processing and extraction of resting state timeseries

The pre-processing of neural images was mainly based on the toolbox Data Processing Assistant for Resting-State fMRI (DPARSF) and some functions in the REST software (REST) and the statistical parametric mapping software (SPM) [30]. DPARSF provides a user-friendly "pipeline" for data analysis of R-fMRI datasets, including noise signal reduction, image normalization and extracting time courses from regions of interest, etc. In general, to assure signal equilibrium and the participant adapting well to the scanning environment, the first few volumes of each of the R-fMRI images should be discarded. Each dataset was corrected for head movement by realignment and regression and any subjects presenting excessive motion (greater than 3.0 mm of translation or 3.0 degrees of rotation in any dimension) were discarded. Given that each researcher had originally discarded the first 5 time points of these selected R-fMRI datasets, we did not remove any volumes during the following preprocessing with DPARSF. First, the R-fMRI time series datasets were separately corrected for slice timing because of different time points used by the three laboratories, with the temporal middle volume as a reference. Second, the images from each subject were spatially normalized into Montreal Neurological Institute (MNI) space using unified segmentation on the T1 image, which requires three steps in DPARSF – coregistration, segmentation and writing normalization parameters. After normalization, spatial smoothing was performed. Third, the systematic drift or trend of the blood oxygen level-dependent (BOLD) signal was removed using a linear model and a band-pass filter (0.009 Hz ~ 0.08 Hz) was applied to the BOLD signal to reduce the effect of both low-frequency and high-frequency physiologic noise. Finally, from the filtered data, using a default mask, we regressed out the effect of nuisance covariates including head motion parameters, global mean signal, white matter signal and cerebrospinal fluid signal.

The preprocessed R-fMRI datasets above were then parcellated into 90 regions, defined by the Automated Anatomic Labeling atlas, to extract the mean time series by averaging all the voxels in each region of interest (ROI) throughout the whole brain [31]. After manually and automatically examining all the process of preprocessing and the mean timeseries, we selected 206 subjects in total for our following analysis.

2.4 Construction of the R-fMRI network

To examine functional connectivity and network characteristics, an interregional correlation matrix (90 X 90, after Fisher z-transformation) was obtained for each of the 206 subjects by calculating the Pearson's correlation coefficients between all possible pairs of the AAL regions. According to Table 1, each average group of correlation matrices was then created by averaging each corresponding correlation Z value throughout each group, thus generating 7 representative correlation matrices. Then, these correlation matrices were thresholded to create adjacency matrices, the element of which is either 1 if the z value is greater than the selected threshold or 0 if it is not. To accurately reflect the alterations in the R-fMRI network, sparsity (S), instead of the same correlation threshold, was applied to thresholding the correlation matrices above, assuring that the network had the same number of edges. In this study, the sparsity is the ratio of the

number of existing edges of the R-fMRI network and the possible maximum edges (90 X 89/2 =4005). e.g., if the sparsity was 5%, it means that the network had 200 edges. A wide range of sparsity (6% ≤ S ≤ 30%) was used to threshold the correlation matrices and estimate the functional connectivity in the fully connected network. Furthermore, we investigated the other graph characteristics with a fixed sparsity (15%) [32]. Finally, the R-fMRI networks were created, in which nodes represent the AAL regions and edges represent functional connections between regions.

2.5 Small world analysis of the R-fMRI network

The small-world organization of a network was originally described by Watts and Strogatz [11] and is characterized by a higher local clustering and a shorter path length. In this study, the clustering coefficient (Cp) is the average of the clustering coefficient over the 90 AAL regions, where the clustering coefficient of the region i (Ci) is defined as the proportion of edges among the immediately connected neighbors of a region divided by the number of edges that could possibly exist between them. The absolute path length (Lp) is the average of the mean shortest absolute path length over the 90 AAL regions of our brain network, where the mean shortest absolute path length of a region i (Li) is defined as the total shortest absolute path length between node I and all the others are divided by N-1 (i.e., 90 - 1). Given that isolated areas may exist in the network and that we would like to explore the small-world parameters throughout a wide range of sparsity values, we used δ ($\delta = 2^{-Lp}$) to indicate the absolute path length between two regions.

2.6 Analysis of the degree correlations in the R-fMRI network

To investigate the difference between the young adulthood network and the late adulthood network from the aspects of degree, we estimated the correlation between each node's degree (K) and the average degree of its direct neighbors (Ki) throughout the 7 representative correlation matrices with a sparsity of 15%. The same parameters of matched random networks, the average over 200 random networks with the same node and degree, were calculated. The linear trend of each group was calculated.

2.7 The functional connectivity within anatomically distinct brain regions

Prior studies suggest that anatomically distinct brain regions are functionally connected. In this study, we investigated the graphic alteration of R-fMRI from young adulthood to late adulthood, in which the above 90 AAL brain regions were anatomically assigned to seven brain areas, i.e., the central region, the frontal lobe, the temporal lobe, the parietal lobe, the occipital lobe and the insula/sub cortical gray nuclei. Due to having only one node of insula, for the convenience of analysis, it was incorporated into the sub cortical gray nuclei and they were grouped into the insula/sub cortical gray nuclei. First, the connections within each brain area, grouped by the above criteria, were calculated throughout all of the individuals. By using this method, we attempted to discover whether there were significant changes of connectivity density within each

anatomically distinct brain region. Second, we estimated the average node strength within each brain area, with the sum of the correlation coefficients (Z value) within corresponding brain areas being divided by the total node number in that brain area.

3. Results

3.1. Data

The demographic data for the young adulthood and the late adulthood groups are shown in Table 1. To assure mutual authentication and to overcome the problem of imbalanced data, we performed all the analyses based on the datasets shown in Table 1, in which the participants were grouped by the original experimenters. Besides, we technologically accommodated this issue with Bootstrapping in the selected part to further verify our results.

3.2 Brain functional networks in young adulthood are more easily fully connected than those in late adulthood'

We first examined the characteristics of 7 representative interregional correlation matrices by calculating the Pearson correlation matrix (R) and its corresponding Fisher-transformation matrix (Z). (See materials and methods). As shown in Table 2, after sorting by correlation coefficient (R/Z) in descending order, the minimum number of edges required to assure that all the Anatomical Automatic Labeling (AAL) regions are fully connected in late adulthood is significantly greater than in young adulthood'(Z value matrix: 275 vs 123±17.3; R value matrix: 276 vs 121±16.1). In addition, we discovered that the corresponding minimum values of correlation coefficients in late adulthood are significantly lower than the minimum correlation coefficients in young adulthood (Z value: 0.38 vs 0.62±0.02, R value: 0.29 vs 0.53±0.01). Furthermore, we explored a correlation coefficient (R/Z) in young adulthood and late adulthood, by keeping the edges the same among the groups (Z value matrix: 275 edges; R value matrix: 276 edges). As predicted, the corresponding minimum correlation coefficients, when keeping the same edges among all the groups, in late adulthood were also markedly lower than in young adulthood (Z value: 0.33 vs 0.44±0.01; R value: 0.29 vs 0.40±0.01). To confirm this result, we drew the correlation coefficient pattern (see Figure S1). Importantly, all the above criteria showed separately obvious distinctions between all the young adulthood groups and the late adulthood group, as opposed to just the average values between the young adulthood groups (As shown table 2).

To explore these differences, we further examined the node frequency of each of the AAL regions of a representative network from Munchen and Leiden Part1, as shown in figure 1A. After sorting by node frequency in descending order, we discovered that the values of approximately 20 of the AAL regions in late adulthood were apparently higher than in young adulthood. As shown in figure 1B, these regions are primarily located in four brain areas, i.e., central regions (4/6, precentral gyrus.L, precentral gyrus.R, postcentral gyrus.L, postcentral gyrus.R), the frontal lobe (7/24, superior frontal gyrus, dorsolateral.L, superior frontal gyrus, dorsolateral.R, middle frontal.L, middle frontal.R, Inferior frontal gyrus, opercular part.R, supplementary motor area.L, supplementary motor area.R), the parietal lobe (4/10, superior parietal gyrus.L, superior parietal gyrus.R, IPL.L, IPL.R) and the limbic lobe (median cingulated and paracingulat.L). It is worth noting that the highest proportion is located in central regions and most regions in the frontal lobe and

that the least and lowest proportion of regions were located in the limbic lobe.

These results suggest that the brain functional network in late adulthood is less likely to be fully connected than that in young adulthood', with a higher node frequency of the 20 AAL regions mainly located in the central regions, the frontal lobe, the parietal lobe and the limbic lobe.

3.3 Comparison of small-world metrics in young adulthood and late adulthood

The human brain is a complicated system, showing extraordinary abilities to rapidly transmit, integrate and precisely process information derived from either the external environment or the organism's internal environment. A small-world network, to some extent, meets this particular requirement with higher clustering coefficients than random networks and similar shortest absolute path length to random networks, and a small-world network has high global and local efficiency with low cost. Over a wide range of sparsity values ($6\% \leq S \leq 30\%$), the clustering coefficients and absolute path lengths of brain functional networks in each participant throughout all the groups were calculated. As shown in figure 2, compared with a matched random network, all the cortical networks (both the late adulthood group and the young adulthood groups) showed similarly identical absolute path lengths ($\lambda \approx 1$, as a few regions in some individuals were not included in the network in case where $6\% \leq \lambda \leq 8\%$, and the value of λ was slightly lower than 1). The cortical networks also showed larger clustering coefficients ($\gamma > 2$). Importantly, the γ values among all the young adulthood groups were apparently higher than for the late adulthood group over a wide range of sparsity values. Additionally, we investigated the clustering coefficient and the absolute path length among all the groups. As shown in figure 2, the clustering coefficient was higher for the late adulthood groups and the absolute path length was lower for the young adulthood groups. As in the prior studies, our findings suggest that the brain functional network had a further loss of small-world characteristics between young adulthood (~20 y) and late adulthood (~60 y).

3.4 Late adulthood exhibits a more social-like organization for brain functional networks than young adulthood

To examine assortative mixing in task-related brain activation, Eguiluz and his colleagues discovered a positive correlation between a node's degree and the average degree of its direct neighbors. This property is not typical of biological networks but is rather distinctive of social networks [22]. As shown in Figure 3, with the data of the late adulthood group (Munchen) and a young adulthood group (Leiden Part1), we calculated each node's degree and average degree of its neighbors for two brain functional networks and 200 matched random networks. Our findings showed that random networks did not present any correlation between node degree and neighbor degree ($C = -0.16$, $R^2 = 0.57$); nevertheless, both of the two brain functional networks clearly presented a positive correlation. Importantly, the network for the late adulthood group ($C = 0.51$, $R^2 = 0.57$) showed a more positive correlation for node degree and neighbor degree than the young adulthood group ($C = 0.17$, $R^2 = 0.65$). As shown in the upper right of Figure 3, a few regions in the late adulthood group with higher degree (> 20) tended to connect with other well-connected nodes, primarily influencing the characteristics of positive correlation compared with

the young adulthood group. After examining these regions with the 20 AAL regions mentioned above, we discovered that the overlap was very common in the central regions, the frontal lobe and the parietal lobe. To confirm this result, we applied the same method to the other groups (Figure S2).

Furthermore, we calculated correlations (C), as mentioned above, of the late adulthood group (Munchen) and the other five young adulthood group with Boostrapping, in which 11 subjects were respectively resampled from each group and then the average networks were constructed as above. The above process was repeated 100 times and the results showed C in late adulthood group was significantly ($p < 0.05$) higher than that in each young late adult group.

As in prior studies, our findings provided additional support for the hypothesis that brain functional networks exhibit the typical properties of social networks, with a highly connected node tending to connect to other well connected nodes, rather than the properties of biological networks. Furthermore, we found that the late adulthood group exhibited a more social-like organization of the brain functional network than the young adulthood group, partly due to a few AAL regions located in the central regions, the frontal lobe and the parietal lobe, where these regions had a higher node degree.

3.5 Comparison of connectivity within anatomically distinct brain areas in the young adulthood groups and the late adulthood group

To assess functional connectivity, there are three widely used methods: seed-based, ICA (independent components analysis) and graph theory. Here, to analyze intrinsic connectivity networks (ICNs) and facilitate group comparisons, we considered the third method: graph theory.

First, all the AAL regions were anatomically assigned to seven brain areas: central regions, the frontal lobe, the temporal lobe, the parietal lobe, the occipital lobe, the limbic lobe and the insula/sub cortical gray nuclei, as shown in Table 3. With a 15% sparsity value, we illustrated the brain functional network map of the representative network of the Munchen group and the Leiden Part1 group, with the different colors representing different brain areas and different node sizes representing different degrees (See Figure 4 and Table S1). As shown in Figure 4, the topological properties of a few regions changed significantly from young adulthood to late adulthood, such as the paracentral lobule.L, paracentral lobule.R, superior parietal gyrus.L, and superior parietal gyrus.R, etc. (L: left, R: right). Second, within each of the anatomically distinct brain areas in each individual throughout the late adulthood group (Munchen) and the young adulthood group (Leiden Part1), the average internal connections and the average node strength were calculated. As shown in Figure 5, the average internal connections of most anatomically distinct brain areas in the Leiden Part1 group were significantly higher than those in late adulthood, such as in the central regions, frontal lobe, temporal lobe, occipital lobe and insula/Sub cortical gray nuclei ($P < 0.01$). Interestingly, only the parietal lobe areas ($P < 0.01$) showed the opposite case. Then, we explored the average node strength within each of the anatomically distinct brain areas. Surprisingly, the node strength showed neither the same pattern nor an opposite pattern with the connection maps mentioned above. There were no significant changes of the average node strength in most of the anatomically distinct brain areas,

such as the central regions, the frontal lobe, the parietal lobe and the insula/sub cortical gray nuclei, etc. there was comparable average node strength within each area (Figure S3, figure S4 and Table S2). Only the average node strength of the occipital lobe ($P < 0.01$) could distinguish between the two age groups.

Furthermore, we calculated average internal connections within each of the anatomically distinct brain areas of the late adulthood group (Munchen) and the other five young adulthood group with Bootstrapping, in which 11 subjects were respectively resampled from each group. The above process was repeated 100 times and the results were compatible with the description above. With the same method, it also presented consistent result for connectivity density.

In summary, we observed that the connectivity density within most of the anatomically distinct brain areas in the young adulthood was significantly higher than that in the late adulthood, except for the parietal lobe, which conversely showed a lower level of connectivity density in young adulthood. Given that we estimated the connectivity density at the same sparsity (15%), which guarantees the same number of connections for networks in young adulthood and late adulthood, our findings indicated that the external interconnections travelling out of the anatomically distinct brain areas should increase from young adulthood to late adulthood. Our finding is compatible with the findings of previous studies. Additionally, our results showed that the average node strength in young adulthood and late adulthood were comparable for most anatomically distinct brain areas, except for the occipital lobe. As shown in Table 2 and Figure S1, the total correlation coefficient in late adulthood was significantly lower than in young adulthood. Therefore, the strength of interconnections traveling out of the anatomically distinct brain areas should become weaker from young adulthood to late adulthood.

4. Discussion

Resting state functional magnetic resonance imaging (R-fMRI) detecting spontaneous low-frequency BOLD signal fluctuations in the human brain, along with graph theory, allowed for the examination of age-related changes of functional connectivity between young adulthood and late adulthood. In the current study, we applied several graph-theoretical metrics, e.g., clustering coefficient, average shortest path, connectivity density, correlation coefficient, etc., to characterize and measure brain functional organization in young adulthood and late adulthood. The main findings of our study were as follow: 1) considering the processes for constructing a functional network, brain functional networks in late adulthood are more difficult to fully connect than those in young adulthood, with a lower average correlation coefficient and higher degree regions mainly located in the central regions, the frontal lobe, the parietal lobe and the limbic lobe; 2) the functional networks in young adulthood and in late adulthood both showed “small-world”-like properties, whereas loss in the small-world characteristics occurred from young adulthood to late adulthood; 3) compared to young adulthood, functional brain networks in late adulthood exhibited a more social-like organization; 4) the connectivity density within most anatomically distinct brain areas showed significantly differences between young adulthood and late adulthood; however, for connectivity strength only two out of the seven regions showed a significant difference.

Overall, our findings provided additional new insights into the aging of brain functional networks. In the following sections, these results are discussed further.

Prior studies have suggested that age-related overactivations were caused by less use of neural

resources, for which one of persuasive explanation was the compensation hypothesis which claims that the network in elderly individuals has to work harder to make up for either its own declining function or to process deficiencies elsewhere in the brain. More recent studies have shown that the human connectome follows an inverted U-shape pattern of connectivity throughout a life span, with an increasingly integrated functional network occurring over the course of development, followed by a plateau lasting for the majority of adulthood and an increasingly localized topology in late life [9,33]. In the current study, we found that some regions located mainly in the central regions, the frontal lobe, the parietal lobe and the limbic lobe showed to be more 'active' (i.e., higher connection number) in late adulthood and were similar to the regions displaying the compensation effect mentioned above. This suggests that these regions had a greater influence on the dynamic changes of functional networks in late adulthood. Moreover, overactivation was largely observed in late adulthood, frequently in prefrontal sites [34], and this prefrontal overactivation was accompanied by medial temporal lobe underactivation [35,36], which was consistent with our findings that a mass of regions located in the frontal lobe were more 'active' and that all regions located in the occipital lobe were 'inactive' (lower connection number). We speculated that these more 'active' regions, mainly located in the central regions, the frontal lobe, the parietal lobe and the limbic lobe occupied more resources in late adulthood, perhaps partly due to a compensatory function, where that the functional network showed a loss of integrated topology and an increased localized topology. However, this explanation has not yet been considered directly. Because we identified 'active' regions in late adulthood and further proposed the above explanation, we expect that this possibility will be addressed in future studies.

The small-world network organization was originally described by Watts and Strogatz [11] and is characterized by a higher local clustering and a shorter path length. This small-world topology was shown to allow higher rates of information processing and learning, which meets the requirements of functional segregation and functional integration for rapidly combining specialized information from distributed brain regions. Collectively, the small-world properties of a brain functional network are conserved throughout the life span – from early childhood to young adulthood and into late adulthood [9,10,12,15]. We confirmed this small-world property in both young adulthood and late adulthood using several data sets and further noted that the functional network had a slight loss in the small-world characteristics from young adulthood to late adulthood. These results are consistent with prior studies [20,21]. Although numerous studies have investigated the relationship between small-world characteristics and development, there was a lack of a definitive understanding of the biological interrelationship between them. We believe that this issue deserves to be further addressed to better understand the dynamic changes of functional networks during aging.

Many complex networks consist of a number of modules that have dense intra-modular connectivity but with relatively sparse inter-modular connectivity. Since Girvan and Newman introduced the concept of modularity, graph-partitioning problems have attracted extensive attention. Collectively, it was clear that brain networks had a modular organization [2,37]. After investigating the modular structure of functional networks, David Meunier and colleagues demonstrated that both young and older brain networks had significant non-random modularity, both of which could be decomposed into three major modules: the superior central, posterior and dorsal fronto-striato-thalamic modules [38]. Briefly, analyzing the degree correlation of a

network could predict its modularity. Based on this approach, Eguiluz et al. and Luca et al. showed a positive correlation between a node's degree and the average degree of its direct neighbors in a functional network. Using the same methods, we estimated this correlation in young adulthood and late adulthood. Our findings confirmed those observations and further showed a higher correlation in late adulthood than in young adulthood. After a basic analysis, we thought that those regions shown to be 'active' should mainly account for the change from young adulthood to late adulthood. However, this analysis provided only a qualitative analysis for modularity in the network. In summary, we provided a new insight into the modularity of functional networks between young adulthood and late adulthood.

Shirer W.R et al. reported that the human brain could be intrinsically organized into fourteen distinct function networks, e.g., auditory, secondary visual cortex (V2) and language, etc. [39]. Numerous studies explored the functional connectivity within and between these networks, collectively indicating an increase in internetwork connections and a decrease in intra-network connections from younger to older, showing a less distinct or dedifferentiated property with advancing aging [27,40-42]. Specifically, a recent study showed that there was a general decrease in correlation strength between regions close in space and an increase in correlation strength between regions more distant in space from children to young adults [9]. In the current study, we examined the connectivity density and connectivity strength within anatomically distinct brain areas. Synthesizing several experimental results, we discovered that most anatomically distinct brain areas (6/7) could significantly distinguish between young adulthood and late adulthood through connectivity density and that a few anatomically distinct brain areas (2/7) could effectively distinguish between age group by connectivity strength. Furthermore, for connectivity density there was a general decrease in density throughout most of the brain areas (central regions, temporal lobe, occipital lobe, limbic lobe, insula/sub cortical gray nuclei) but an increase within the parietal lobe with advancing aging. For connectivity strength, the temporal lobe and the occipital lobe showed a decrease in strength from young adulthood to late adulthood. Our findings were compatible with prior reports that functional brain networks in the elderly become less distinct. Here, our results further showed that the temporal lobe, involved in auditory/language functions, presented an opposite change (for connectivity density and connectivity strength), that the occipital lobe, involved in visual processing, presented a similar change and that others presented other patterns. Although, a more recent study explored age-related changes in functional connectivity and showed that connectivity decreased with age within the default mode, the cingulo-opercular and fronto-parietal control networks, connectivity was conserved within the somatomotor and visual networks. We believed that this functional connectivity analysis, using our measures and anatomically distinct brain areas, will be meaningful for understanding the dynamic changes of the functional networks. We expect a future research to further elucidate our findings.

Conclusion

In the current study, we confirmed that human brain functional networks, studied by R-fMRI, presented a further loss of small-world characteristics from young adulthood to late adulthood. Moreover, our findings suggest that brain functional networks in young adulthood are more easily fully connected than those in late adulthood, possibly due to several regions in late adulthood occupying more resources, such as the frontal lobe, central regions, the parietal lobe

and the limbic lobe. Additionally, our results implied that late adulthood exhibited a more social-like organization for brain functional networks than that in young adulthood. Finally, we showed that the connectivity density of most of the anatomically distinct brain areas presented a general decrease in density and that the connectivity strength of the temporal lobe and the occipital lobe presented a decrease in strength from young adulthood to late adulthood. However, considering these two measures, there are some different patterns of variability. Together with other observations, we believed that our findings would be useful for further understanding the brain aging process.

Conflict of Interests

The authors declare that there is no conflict of interests regarding the publication of this paper.

Acknowledgments

We thank Francine Dai, Lu Zhang and Changwei Lei for helpful discussions and correction of the writing. This work was funded by the National Natural Science Foundation of China (No. 21375090 and 21175095).

References

1. Stranahan AM, Mattson MP (2012) Recruiting adaptive cellular stress responses for successful brain ageing. Nat Rev Neurosci 13: 209-216.
2. Bullmore E, Sporns O (2009) Complex brain networks: graph theoretical analysis of structural and functional systems. Nat Rev Neurosci 10: 186-198.
3. Giorgio A, Watkins KE, Douaud G, James AC, James S, et al. (2008) Changes in white matter microstructure during adolescence. Neuroimage 39: 52-61.
4. Cascio CJ, Gerig G, Piven J (2007) Diffusion tensor imaging: Application to the study of the developing brain. J Am Acad Child Adolesc Psychiatry 46: 213-223.
5. Dennis EL, Thompson PM (2014) Functional brain connectivity using fMRI in aging and Alzheimer's disease. Neuropsychol Rev 24: 49-62.
6. Biswal B, Yetkin FZ, Haughton VM, Hyde JS (1995) Functional connectivity in the motor cortex of resting human brain using echo-planar MRI. Magn Reson Med 34: 537-541.
7. Fox MD, Raichle ME (2007) Spontaneous fluctuations in brain activity observed with functional magnetic resonance imaging. Nat Rev Neurosci 8: 700-711.
8. Jolles DD, van Buchem MA, Crone EA, Rombouts SA (2011) A comprehensive study of whole-brain functional connectivity in children and young adults. Cereb Cortex 21: 385-391.
9. Fair DA, Cohen AL, Power JD, Dosenbach NU, Church JA, et al. (2009) Functional brain networks develop from a "local to distributed" organization. PLoS Comput Biol 5: e1000381.
10. Supekar K, Musen M, Menon V (2009) Development of large-scale functional brain networks in children. PLoS Biol 7: e1000157.
11. Watts DJ, Strogatz SH (1998) Collective dynamics of 'small-world' networks. Nature 393: 440-442.
12. Achard S, Salvador R, Whitcher B, Suckling J, Bullmore E (2006) A resilient, low-frequency, small-world human brain functional network with highly connected association cortical hubs. J Neurosci 26: 63-72.
13. Bassett DS, Meyer-Lindenberg A, Achard S, Duke T, Bullmore E (2006) Adaptive reconfiguration of fractal small-world human brain functional networks. Proc Natl Acad Sci U S A 103: 19518-

19523.

14. Smit DJ, Stam CJ, Posthuma D, Boomsma DI, de Geus EJ (2008) Heritability of "small-world" networks in the brain: a graph theoretical analysis of resting-state EEG functional connectivity. Hum Brain Mapp 29: 1368-1378.
15. Supekar K, Menon V, Rubin D, Musen M, Greicius MD (2008) Network analysis of intrinsic functional brain connectivity in Alzheimer's disease. PLoS Comput Biol 4: e1000100.
16. Sanz-Arigita EJ, Schoonheim MM, Damoiseaux JS, Rombouts SA, Maris E, et al. (2010) Loss of 'small-world' networks in Alzheimer's disease: graph analysis of FMRI resting-state functional connectivity. PLoS One 5: e13788.
17. Liu Y, Liang M, Zhou Y, He Y, Hao Y, et al. (2008) Disrupted small-world networks in schizophrenia. Brain 131: 945-961.
18. Lynall ME, Bassett DS, Kerwin R, McKenna PJ, Kitzbichler M, et al. (2010) Functional connectivity and brain networks in schizophrenia. J Neurosci 30: 9477-9487.
19. Zhang J, Wang J, Wu Q, Kuang W, Huang X, et al. (2011) Disrupted brain connectivity networks in drug-naive, first-episode major depressive disorder. Biol Psychiatry 70: 334-342.
20. Achard S, Bullmore E (2007) Efficiency and cost of economical brain functional networks. PLoS Comput Biol 3: e17.
21. Onoda K, Yamaguchi S (2013) Small-worldness and modularity of the resting-state functional brain network decrease with aging. Neurosci Lett 556: 104-108.
22. Eguiluz VM, Chialvo DR, Cecchi GA, Baliki M, Apkarian AV (2005) Scale-free brain functional networks. Phys Rev Lett 94: 018102.
23. Soffer SN, Vazquez A (2005) Network clustering coefficient without degree-correlation biases. Phys Rev E Stat Nonlin Soft Matter Phys 71: 057101.
24. Ferrarini L, Veer IM, Baerends E, van Tol MJ, Renken RJ, et al. (2009) Hierarchical functional modularity in the resting-state human brain. Hum Brain Mapp 30: 2220-2231.
25. Koch W, Teipel S, Mueller S, Buerger K, Bokde AL, et al. (2010) Effects of aging on default mode network activity in resting state fMRI: does the method of analysis matter? Neuroimage 51: 280-287.
26. Damoiseaux JS, Beckmann CF, Arigita EJ, Barkhof F, Scheltens P, et al. (2008) Reduced resting-state brain activity in the "default network" in normal aging. Cereb Cortex 18: 1856-1864.
27. Geerligs L, Renken RJ, Saliasi E, Maurits NM, Lorist MM (2014) A Brain-Wide Study of Age-Related Changes in Functional Connectivity. Cereb Cortex.
28. Chan MY, Park DC, Savalia NK, Petersen SE, Wig GS (2014) Decreased segregation of brain systems across the healthy adult lifespan. Proc Natl Acad Sci U S A 111: E4997-5006.
29. Menon V (2011) Large-scale brain networks and psychopathology: a unifying triple network model. Trends Cogn Sci 15: 483-506.
30. Chao-Gan Y, Yu-Feng Z (2010) DPARSF: A MATLAB Toolbox for "Pipeline" Data Analysis of Resting-State fMRI. Front Syst Neurosci 4: 13.
31. Tzourio-Mazoyer N, Landeau B, Papathanassiou D, Crivello F, Etard O, et al. (2002) Automated anatomical labeling of activations in SPM using a macroscopic anatomical parcellation of the MNI MRI single-subject brain. Neuroimage 15: 273-289.
32. Stam CJ, Jones BF, Nolte G, Breakspear M, Scheltens P (2007) Small-world networks and functional connectivity in Alzheimer's disease. Cereb Cortex 17: 92-99.
33. Collin G, van den Heuvel MP (2013) The ontogeny of the human connectome: development and

dynamic changes of brain connectivity across the life span. Neuroscientist 19: 616-628.
34. Cabeza R, Daselaar SM, Dolcos F, Prince SE, Budde M, et al. (2004) Task-independent and task-specific age effects on brain activity during working memory, visual attention and episodic retrieval. Cereb Cortex 14: 364-375.
35. Gutchess AH, Welsh RC, Hedden T, Bangert A, Minear M, et al. (2005) Aging and the neural correlates of successful picture encoding: frontal activations compensate for decreased medial-temporal activity. J Cogn Neurosci 17: 84-96.
36. Grady CL, McIntosh AR, Craik FI (2003) Age-related differences in the functional connectivity of the hippocampus during memory encoding. Hippocampus 13: 572-586.
37. Meunier D, Lambiotte R, Fornito A, Ersche KD, Bullmore ET (2009) Hierarchical modularity in human brain functional networks. Front Neuroinform 3: 37.
38. Meunier D, Achard S, Morcom A, Bullmore E (2009) Age-related changes in modular organization of human brain functional networks. Neuroimage 44: 715-723.
39. Shirer WR, Ryali S, Rykhlevskaia E, Menon V, Greicius MD (2012) Decoding subject-driven cognitive states with whole-brain connectivity patterns. Cereb Cortex 22: 158-165.
40. Geerligs L, Maurits NM, Renken RJ, Lorist MM (2014) Reduced specificity of functional connectivity in the aging brain during task performance. Hum Brain Mapp 35: 319-330.
41. Carp J, Park J, Polk TA, Park DC (2011) Age differences in neural distinctiveness revealed by multi-voxel pattern analysis. Neuroimage 56: 736-743.
42. Dennis NA, Cabeza R (2011) Age-related dedifferentiation of learning systems: an fMRI study of implicit and explicit learning. Neurobiol Aging 32: 2318 e2317-2330.

Figure Legends

Figure 1. The degree distribution of the exactly right fully connected functional network.

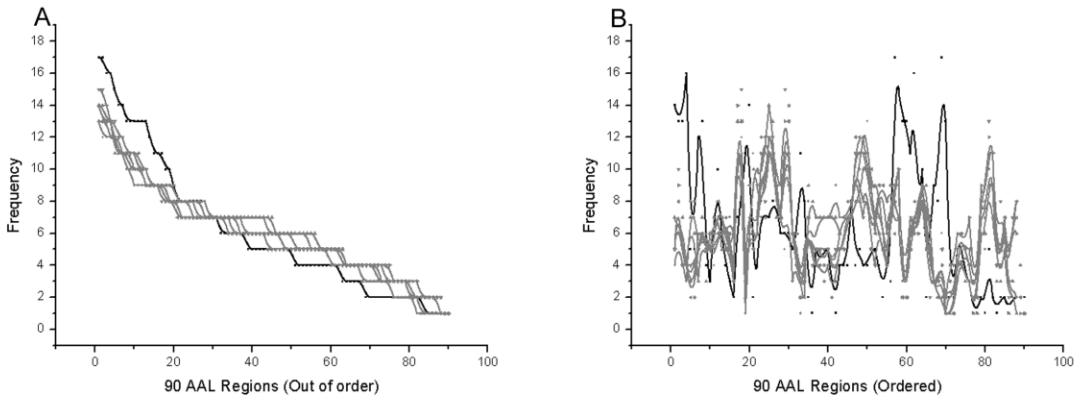

The degree distributions of the mean functional network were mapped, during which all of the regions in the late adulthood group were rightly included and the young adulthood networks had the same edges. **A –** The region was sorted by its degree in descending order. The black line represents the degree distribution of the late adulthood group and the grey lines represent the degree distribution in the young adulthood groups. **B –** The region was ordered by the rules in table S3. As above, the lines represent the corresponding groups. The regions possessing the highest degree, approximately 20 regions, showed a higher degree in the late adulthood group

than in the young adulthood groups. These regions were mainly located in the central regions, the frontal lobe, the parietal lobe and the limbic lobe.

Figure 2. Small-world properties of the brain functional network.

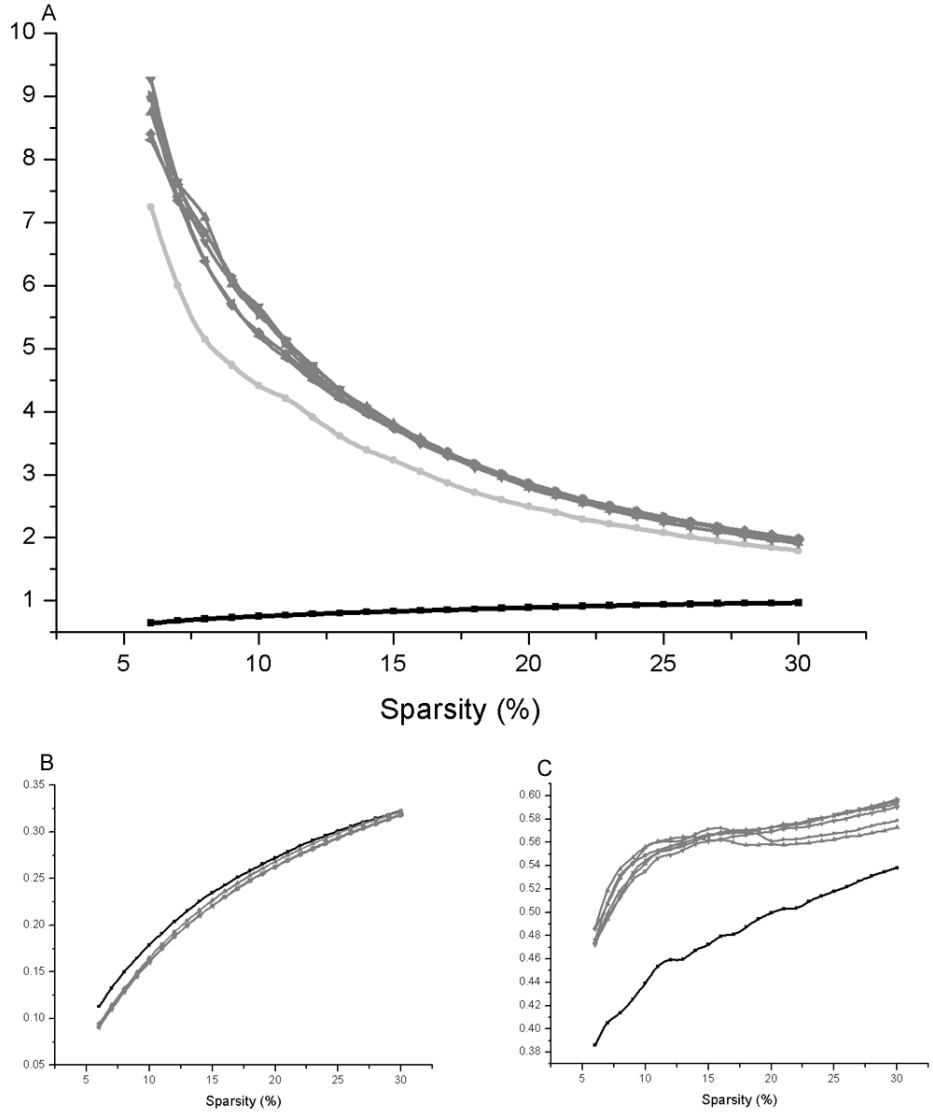

In this figure, the mean absolute path lengths (Lambda $\lambda = \delta^{real}/\delta^{rand}$) and mean clustering coefficients (Gamma $\gamma = Cp^{real}/Cp^{rand}$) were calculated from each matrix over a wide range of sparsity values ($6\% \leq S \leq 30\%$). For details see Materials and Methods. **A –** All the networks showed $\gamma > 1$ (the light grey line and dark grey lines) and $\lambda \approx 1$ (the black line), which indicated small-world properties. **B -** The black line represents the mean clustering coefficient in late adulthood and the grey lines represent the mean clustering coefficient in young adulthood. **C –** The black line represents the mean absolute path length in late adulthood and the grey lines represent the mean absolute path length in young adulthood. The young adulthood data have a higher γ value over a wide range of sparsity values. The mean absolute path length was shorter in young adulthood and the mean clustering coefficient was lower in young adulthood.

Figure 3. Comparison of the correlation between the degree of each region and its direct neighbors.

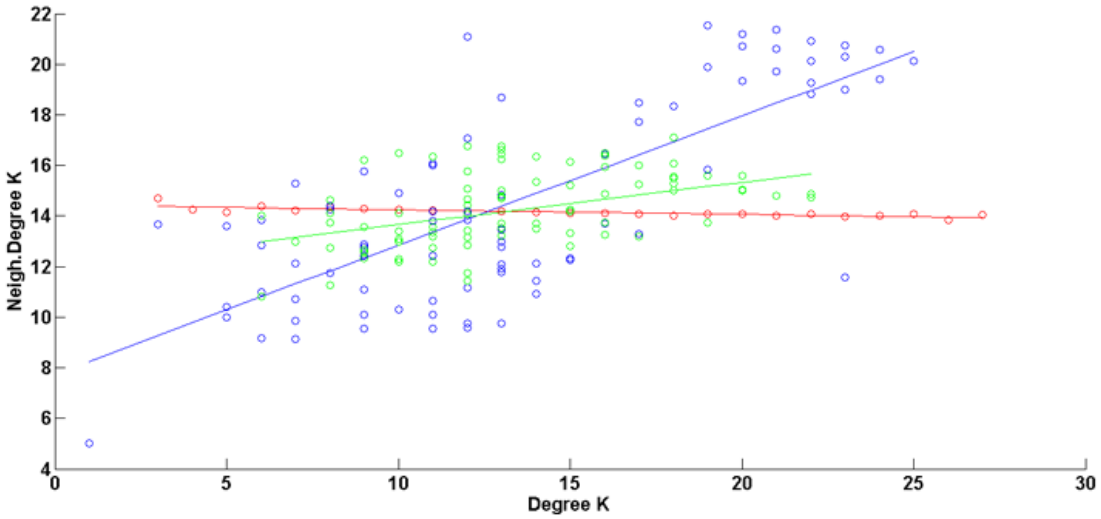

In this figure, the correlation between the degree of each region and its direct neighbors was estimated based on the mean network, with a sparsity value (15%) from the mean correlation matrix of young adulthood and late adulthood. Averaging over 200 random networks (in green) did not show any correlation. Conversely, the brain functional network in young adulthood (in red) and late adulthood (in blue) both showed a significant positive correlation between degree and neighbor degree. Moreover, this correlation is present more strongly in late adulthood, perhaps intuitively due to the regions in the upper right of the figure.

Figure 4. Graphical visualization of the brain functional networks in young adulthood and late adulthood.

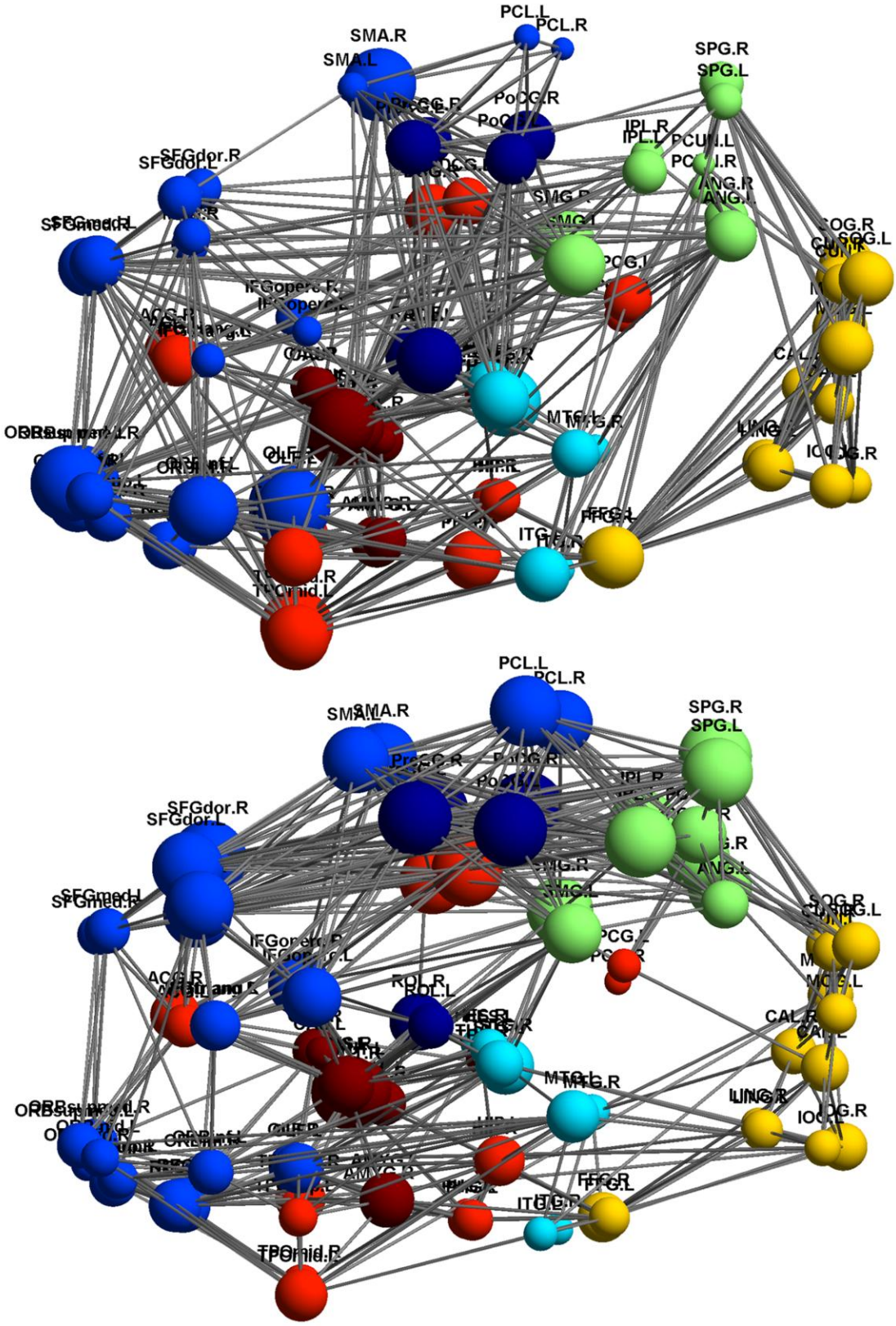

The graph was drawn based on the mean functional network of young adulthood and late adulthood. Each node represents an AAL region. The size of the nodes indicates their degrees. The color of the nodes indicates an anatomical location: central regions (dark blue), frontal lobe (blue), temporal lobe (light blue), parietal lobe (green), occipital lobe (yellow), limbic lobe (blood

red), insula/sub cortical gray nuclei (crimson). (See details in table S1).

Figure 5. The comparison of functional connectivity within anatomically distinct brain areas.

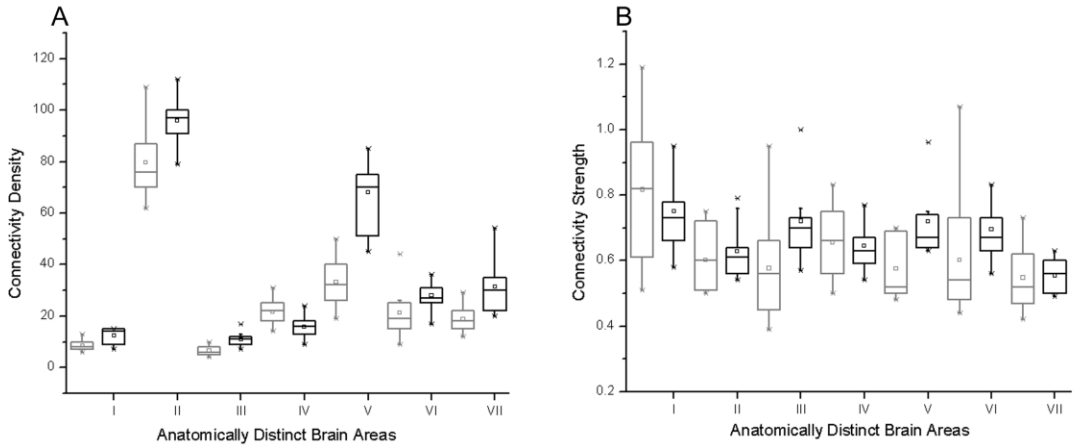

The connectivity density and connectivity strength within anatomically distinct brain areas were separately calculated through each participant. **A –** The connectivity density within anatomically distinct brain areas was calculated in young adulthood (in black box) and late adulthood (in grey box) (y-axis, connectivity density; x-axis, seven anatomically distinct brain areas). **B –** The connectivity strength within anatomically distinct brain areas was separately calculated. As above, the boxes represent corresponding groups (y-axis, connectivity strength; x-axis, seven anatomically distinct brain areas). Most anatomically distinct brain areas showed a general decrease of connectivity density but no obvious change of connectivity strength. (For details see Results). I: Central region; II: Frontal lobe; III: Temporal lobe; IV: Parietal lobe; V: Occipital lobe; VI: Limbic lobe; VII: Insula/Sub cortical gray nuclei.

Tables

Table 1. Demographic data for the participants

Group	Age	Gender
Munchen (n = 11)	66.64 (rang: 63 to 73, SD: 3.20)	7 males, 4 females
Leiden Part1 (n = 12)	23.00 (rang: 20 to 27, SD: 2.38)	12 males, 0 females
Leiden Part2 (n = 19)	21.68 (rang: 18 to 28, SD: 2.49)	11 males, 8 females
Zang Part1 (n = 40)	21.40 (rang: 18 to 26, SD: 2.10)	17 males, 23 females
Zang Part2 (n = 41)	21.17 (rang: 18 to 26, SD: 1.61)	15 males, 26 females
Zang Part3 (n = 40)	20.98 (rang: 18 to 25, SD: 1.84)	17 males, 23 females
Zang Part5 (n = 43)	21.21 (rang: 18 to 26, SD: 1.80)	15 males, 28 females

Table 2. The minimum edges to assure all the AAL regions could be fully connected

Group	Minimum edges (Z, R)	Minimum Z/R value	275^{th}/276^{th} Z/R value
Munchen	275, 276	0.38, 0.29	0.33, 0.29
Leiden Part1	102, 107	0.65, 0.54	0.44, 0.39
Leiden Part2	144, 144	0.58, 0.51	0.43, 0.39
Zang Part1	102, 102	0.64, 0.55	0.44, 0.39
Zang Part2	116, 113	0.62, 0.53	0.45, 0.40
Zang Part3	133, 120	0.61, 0.53	0.45, 0.40
Zang Part4	141, 141	0.60, 0.52	0.45, 0.41

The connection number and its correlation strength (Z/R) to assure a fully-connected network were estimated.

Table 3. All the AAL regions were anatomically assigned to seven distinct brain areas

Distinct Areas	AAL regions/Nodes
Central regions (I)	PreCG.L, PreCG.R, ROL.L, ROL.R, PoCG.L, PoCG.R
Frontal lobe (II)	SFGdor.L, SFGdor.R, ORBsup.L, ORBsup.R, MFG.L, MFG.R, ORBmid.L, ORBmid.R, IFGoperc.L, IFGoperc.R, IFGtriang.L, IFGtriang.R, ORBinf.L, ORBinf.R, SMA.L, SMA.R, OLF.L, OLF.R, SFGmed.L, SFGmed.R, ORBsupmed.L, ORBsupmed.R, REC.L, REC.R
Temporal lobe (III)	HES.L, HES.R, STG.L, STG.R, MTG.L, MTG.R, ITG.L, ITG.R
Parietal lobe (IV)	SPG.L, SPG.R, IPL.L, IPL.R, SMG.L, SMG.R, ANG.L, ANG.R, PCUN.L, PCUN.R
Occipital lobe (V)	CAL.L, CAL.R, CUN.L, CUN.R, LING.L, LING.R, SOG.L, SOG.R, MOG.L, MOG.R, IOG.L, IOG.R, FFG.L, FFG.R
Limbic lobe (VI)	ACG.L, ACG.R, DCG.L, DCG.R, PCG.L, PCG.R, HIP.L, HIP.R, PHG.L PHG.R, TPOsup.L, TPOsup.R, TPOmid.L, TPOmid.R
Insula/Sub cortical gray neclei (VII)	INS.L, INS.R, AMYG.L, AMYG.R, CAU.L, CAU.R, PUT.L, PUT.R, PAL.L, PAL.R, THA.L, THA.R